

prp8 mutations that cause human Retinitis pigmentosa lead to a U5 snRNP maturation defect in yeast.

Kum-Loong Boon^{1,3}, Richard J. Grainger¹, Parastoo Ehsani¹, J. David Barrass¹, Tatsiana Auchynnikava¹, Chris F. Inglehearn² and Jean D. Beggs¹

¹Wellcome Trust Centre for Cell Biology, University of Edinburgh, King's Buildings, Mayfield Road, Edinburgh EH9 3JR, UK.

²Section of Ophthalmology and Neuroscience, Leeds Institute of Molecular Medicine, University of Leeds, St James's University Hospital, Leeds LS9 7TF, UK. ³ Present address: Center for Molecular Neurobiology, The Ohio State University, 190 Rightmire Hall, 1060 Carmack Road, Columbus, Ohio 43210, U.S.A. Correspondence should be addressed to J.D.B. (jbeggs@ed.ac.uk).

Prp8 protein is a highly conserved pre-mRNA splicing factor and a component of spliceosomal U5 snRNPs. Intriguingly, although it is ubiquitously expressed, mutations in the C-terminus of human Prp8p cause the retina-specific disease Retinitis pigmentosa (RP). The biogenesis of U5 snRNPs is poorly characterized. We present evidence for a cytoplasmic precursor U5 snRNP in yeast that lacks a mature U5 snRNP component, Brr2p, and depends on a nuclear localization signal in Prp8p for its efficient nuclear import. The association of Brr2p with the U5 snRNP occurs within the nucleus. RP mutations in Prp8p in yeast result in nuclear accumulation of the precursor U5 snRNP, apparently as a consequence of disrupting the interaction of Prp8p with Brr2p. We therefore propose a novel assembly pathway for U5 snRNP complexes, which is disrupted by mutations that cause human RP.

Nuclear pre-mRNA splicing is an essential housekeeping process in all eukaryotic cells. It is catalyzed by a large ribonucleoprotein (RNP) complex called the spliceosome, which contains the small nuclear RNPs (snRNPs) U1, U2, U4, U5 and U6, as well as many non-snRNP proteins^{1, 2}. Each snRNP consists of an snRNA, a set of specific proteins, and seven common Sm proteins or, in the case of U6 snRNP, seven Lsm proteins.

Unexpectedly, mutations in four human snRNP-associated proteins, PRPF8³, PRPF31⁴, PRPF3⁵ and PAP-1/RP9^{6, 7} were found in patients with a dominantly inherited form of retinal degeneration, Retinitis pigmentosa (RP). Here, we investigate the role of Prp8p (the yeast ortholog of PRPF8) in U5 snRNP biogenesis in *Saccharomyces cerevisiae*, and the effect of RP mutations on this process.

Biogenesis of the U snRNPs has been studied extensively in metazoans^{1, 8}. The U1, U2, U4 and U5 snRNAs are produced as precursors in the nucleus by RNA polymerase II then exported to the cytoplasm, facilitated by nuclear cap-binding proteins and the export factors, CRM1 and PHAX⁸. In the cytoplasm seven Sm proteins bind to the snRNAs, facilitated by the SMN complex^{9, 10}, and the m⁷G cap is hypermethylated to form a 2,2,7-trimethylguanosine (m₃G) cap¹. This maturation generates a bipartite nuclear localization signal (NLS), composed of the Sm protein complex and the m₃G cap, which permits import of the core snRNP to the nucleus, mediated by the SMN complex, Importin β and Snurportin-1¹¹. Association of snRNP-specific proteins with the core particles is required to produce mature snRNPs. Several U1- and U2-specific proteins are imported to the nucleus independently of their cognate snRNAs, and associate with core snRNPs in nuclear Cajal bodies¹²⁻¹⁵. It is not known at what stage the U5 specific proteins associate with the core snRNP. The biogenesis of U snRNPs in yeast is less well characterized. No orthologs of PHAX or Snurportin-1 have been identified in *S. cerevisiae*^{11, 16}, indicating that the nuclear export and re-import pathway may not exist in yeast.

Prp8p is a large (274 kDa in humans) U5 snRNP-specific protein. It is highly conserved in both sequence and size (reviewed by¹⁷), is essential for pre-mRNA splicing¹⁸ and is produced in all mammalian tissues¹⁹. The human PRPF8 gene consists of 42 exons that encode a 2335 residue protein. Mutations in PRPF8 cause a severe form of dominant RP³. At least sixteen different mutations have been identified to date, including missense changes, premature stops and deletions^{3, 20-24}.

These mutations are clustered at the C-terminus of the protein in a conserved region within the last exon.

In budding yeast, Prp8p associates with U5 snRNA in two complexes. The simpler Aar2-U5 snRNP²⁵ consists of Prp8p, Snu114p, Aar2p, Sm proteins and U5 snRNA. The larger U5 snRNP²⁶ lacks Aar2p, but instead contains Brr2p, Prp28p, Snu40p and Dib1p. It has been suggested that the Aar2-U5 snRNP might represent an intermediate particle in U5 snRNP biogenesis²⁵. Here, we identify a functional NLS in Prp8p and show that in its absence the Aar2-U5 snRNP appears to accumulate in the cytoplasm. In contrast, the nuclear accumulation of Brr2p, a specific component of the larger U5 snRNP, is unaffected. A similar analysis in yeast carrying *prp8* mutations that cause RP in humans also shows an increase in the Aar2-U5 snRNP, however, RP-Prp8 proteins accumulate in the nucleus. We therefore propose a model for U5 snRNP biogenesis and a molecular basis for a splicing defect caused by mutations that lead to RP in humans.

RESULTS

Evidence for a cytoplasmic U5 snRNP

A putative NLS was identified at amino acids (aa) 96–117 of Prp8p of *S. cerevisiae* within a region rich in basic amino acids that is conserved in most eukaryotes¹⁷. Codons 96–117 of *PRP8* were deleted from plasmid pJU204²⁷ to produce pKLANLS (*prp8* Δ NLS-3HA), and these plasmids were introduced into yeast strains KL1 and KL3 (Table 1), in which the chromosomal *P_{GALI}-PRP8* is strongly repressed in glucose medium. pKLANLS supported only slow growth of these cells on glucose (4.5 hours doubling time; data not shown). Immuno-fluorescent staining of cells showed that full-length Prp8p localized to the nucleus, whereas Δ NLS-Prp8p was present in both nucleus and cytoplasm (**Fig. 1a**). When aa96–117 of Prp8p were fused to the N-terminus of GFP this caused the GFP-NLS fusion protein to accumulate in nuclei (**Fig. 1b**), confirming that this region of yeast Prp8p contains a functional NLS. As there was sufficient nuclear Δ NLS-Prp8 protein to support cell viability, albeit with very slow growth, there may be another NLS that allows inefficient nuclear uptake of this very large protein. Candidates include another cluster of basic residues in the N-terminal portion of Prp8p¹⁷ or, by analogy with metazoan systems, the m₃G cap of U5 snRNA and/or the Sm proteins SmB and SmD1 that also have NLSs²⁸.

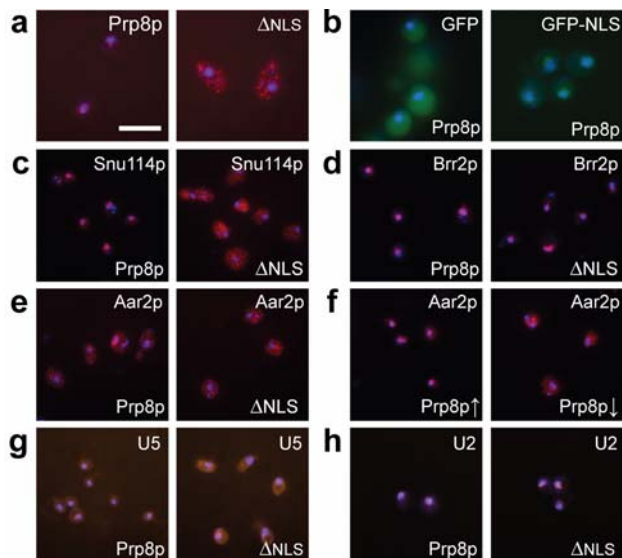


Figure 1 Functional analysis of a nuclear localization signal in Prp8p. (a) Immunofluorescent localization of full-length Prp8-3HAp (Prp8p) and Δ NLS-Prp8-3HAp (Δ NLS) in KL1 cells. (b) Localization of GFP and GFP fused to aa96–117 of Prp8p (GFP-NLS). Immunofluorescent localization of (c) Snu114-TAP, (d) Brr2-TAP, (e) Aar2-TAP in KL1 cells producing either Prp8p or Δ NLS-Prp8p, or (f) Aar2-TAP in KL1 cells grown in YPGR to over-express Prp8p (\uparrow) or shifted into YPDA for 12 h to deplete Prp8p (\downarrow). RNA FISH for (g) U5 snRNA or (h) U2 snRNA localization was performed on KL1 cells producing either Prp8p or Δ NLS-Prp8p. In each panel the protein or RNA being detected is indicated at the top and the status of Prp8p is shown at the bottom. These are merged images: immunofluorescence is shown as red, DAPI is shown as blue, GFP is green. Scale bar, 10 μ m.

Next, pJU204 or pKLANLS was introduced into yeast strains KL1-Aar2, KL1-Brr2 and KL1-Snu114 (in which the indicated protein is TAP-tagged) and the tagged proteins were observed microscopically. In strains with full-length Prp8p, the localization of Snu114p and Brr2p was nuclear, whereas Aar2p was present in both nucleus and cytoplasm (**Fig. 1c–e**). In strains with Δ NLS-Prp8p, Snu114p was delocalized, with a substantial amount present in the cytoplasm (**Fig. 1c**), whereas Brr2p was consistently nuclear (**Fig. 1d**). The cytoplasmic staining of Aar2p was also slightly increased with Δ NLS-Prp8p (**Fig. 1e**), but this effect was difficult to assess. However, when Prp8p was over-expressed, Aar2p became concentrated in the nucleus, whereas upon Prp8p depletion Aar2p was observed throughout the cells (**Fig. 1f**). This suggests that the nuclear accumulations of Prp8p and Aar2p are linked; Prp8p might mediate the nuclear accumulation of Aar2p or vice versa.

Prp8p is a component of U4/U6.U5 tri-snRNPs as well as of free U5 snRNPs. Significantly, Δ NLS-Prp8p co-precipitated the U5 snRNAs almost as efficiently as did full-length Prp8p but co-precipitated less U4 and U6 snRNAs (50–60% compared to full-length Prp8p; **Supplementary Fig. 1a**), suggesting a defect in the incorporation of Δ NLS-Prp8p into tri-snRNPs. Such a defect may occur as a consequence of defective U5 snRNPs or fewer U5 snRNPs in the nucleus. Extract prepared from glucose-grown KL1 cells that depend on Δ NLS-Prp8p for viability also displayed a lower splicing activity (**Supplementary Fig. 1b**), which may be caused by the reduced level of tri-snRNPs.

As the U5 snRNAs appeared to be associated as efficiently with Δ NLS-Prp8p as with full-length Prp8p, despite Δ NLS-Prp8p being distributed throughout the cells, the localization of U5 snRNA was investigated. RNA fluorescent in situ hybridisation (FISH) showed that U5 snRNA was predominantly nuclear in the presence of full-length Prp8p but gave a substantial cytoplasmic signal in the Δ NLS-Prp8p strain

(**Fig. 1g**). It is therefore likely that Δ NLS-Prp8p is associated with U5 snRNA in the cytoplasm as well as in the nucleus. In contrast, U2 snRNA was nuclear in both strains (**Fig. 1h**), as was U6 snRNA (data not shown).

Distinct Aar2- and Brr2-U5 snRNPs

In biochemical studies, human Brr2p (hBrr2p) was found stably associated with hPrp8p in the absence of RNA²⁹. However, a U5 RNP complex has been identified²⁵ that contains Prp8p and Aar2p but not Brr2p. Indeed, we found that TAP-tagged Prp8p pulled down Aar2p (**Fig. 2a**, lane 2), but that TAP-tagged Brr2p did not co-precipitate Aar2p from extract containing either wild-type Prp8p or Δ NLS-Prp8p (**Fig. 2a**, lanes 3,4).

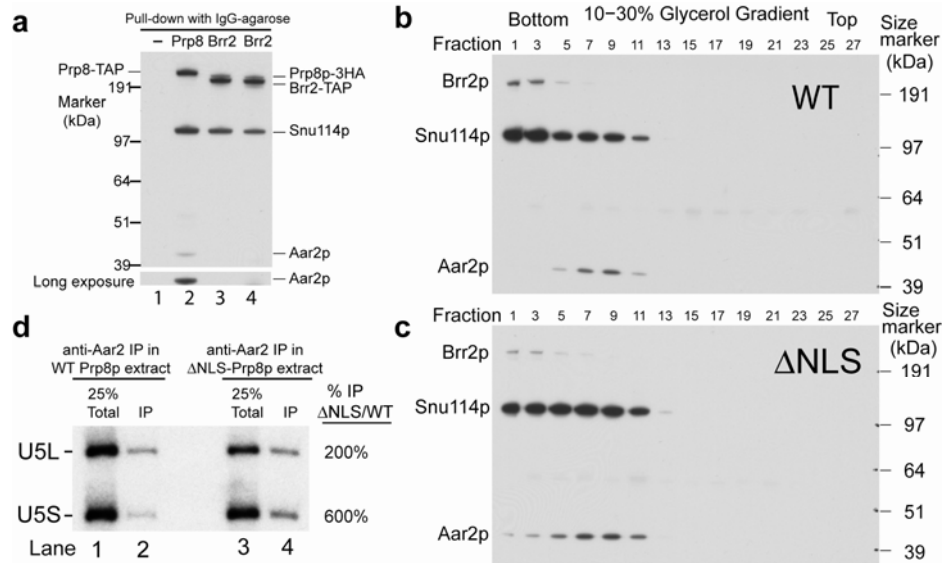
The distribution of Aar2p, Brr2p, and Snu114p in Prp8p-associated complexes was analyzed using a combination of glycerol gradient centrifugation and anti-HA immunoprecipitation of extracts from KL3-Brr2 cells expressing either full-length Prp8-3HAp or Δ NLS-Prp8-3HAp. Gradient fractions were incubated with anti-HA agarose and the precipitates were analyzed by western blotting for the presence of Brr2-13Myc, Snu114p and Aar2p. The results show that Δ NLS-Prp8p co-precipitated more Aar2p and less Brr2p than did wild-type Prp8p (**Fig. 2**). With wild-type Prp8p, Snu114p was more concentrated in the bottom fractions (**Fig. 2b**, fractions 1–5) that contained the Prp8-associated Brr2p, but little or no Aar2p. In contrast, with Δ NLS-Prp8p, Snu114p was more evenly distributed between the fractions containing Brr2p and Aar2p (**Fig. 2c**, fractions 1–11). Thus, the Δ NLS-Prp8p extract contained more Prp8p-Snu114p-Aar2p complex and less Prp8p-Snu114p-Brr2p complex than wild-type.

The association of U5 snRNA with the Aar2p complex was investigated in cell extracts from KL1-Aar2 containing either Prp8p or Δ NLS-Prp8p. As shown in **Figure 2d**, an increased amount of U5 snRNA co-precipitated with Aar2p from extract containing Δ NLS-Prp8p compared to full-length Prp8p. This supports the conclusion from the gradient fractionation experiment that the level of Aar2p-U5 snRNP complex increased when nuclear accumulation of Prp8p was hindered.

Thus, the existence of two distinct Prp8p complexes^{25, 26} is supported by our finding that Prp8p was associated independently with Brr2p or with Aar2p in different glycerol gradient fractions, and that Brr2p did not pull down Aar2p. Furthermore, the glycerol gradient results showing that the *prp8 Δ NLS* mutation increased the amount of Aar2p-Prp8p complex and decreased the amount of Brr2p-Prp8p complex, suggests that these complexes may be in equilibrium. The presence of U5 snRNA in a cytoplasmic Aar2-Prp8p complex is suggested by the delocalization of U5 snRNA and the association of more Aar2p with U5 snRNA and with Prp8p in *prp8 Δ NLS* cells. Also, although Δ NLS-Prp8p is substantially delocalized to the cytoplasm it is nevertheless associated with a similar amount of U5 snRNA compared with full-length Prp8p. We therefore propose that there is a cytoplasmic Aar2-Prp8p-Snu114-U5 snRNP complex that, once imported to the nucleus, is in equilibrium with the Brr2-Prp8p-Snu114-U5 mature snRNP complex.

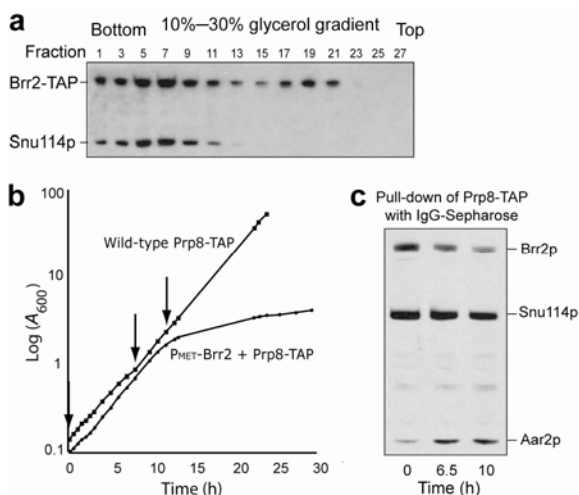
The existence of a U5 precursor that lacks Brr2p raises the question as to whether there is a separate pool of Brr2p that is not Prp8p-associated, or whether Brr2p may be limiting in yeast cells. To investigate this, cell extract containing Brr2-TAP and untagged Prp8p was analyzed by glycerol gradient fractionation, precipitation with IgG-agarose and western blotting with anti-Snu114p antibodies. Interestingly, two peaks of Brr2p were found, one at the bottom of the gradient (**Fig. 3a**, fractions 1 to 11) that co-precipitates Snu114p, and another in lighter fractions (**Fig. 3a**, fractions 17 to 21) that does not co-precipitate

Figure 2. More Prp8p-Aar2-U5 snRNP complex forms with Δ NLS-Prp8p. **(a)** Aar2p is co-immunoprecipitated with Prp8p but not with Brr2p. Cell extracts from non-tagged strain BMA38a (lane 1), Prp8-TAP strain RG8T (lane 2), or Brr2-TAP strain KL1-Brr2 carrying pJU204 (Prp8-3HAp; lane 3) or pKL Δ NLS (Δ NLS-Prp8-3HAp; lane 4) were incubated with IgG-agarose and precipitates were analyzed by western blotting with anti-HA, anti-Aar2 and anti-Snu114 antibodies (N.B. Prp8-TAP in lane 3 and Brr2-TAP in lanes 3 and 4 are detected by any IgG). A longer exposure of the Aar2 region of the blot is shown below. **(b, c)** Glycerol gradient fractionation of Prp8p-HAp-associated complexes from KL3-Brr2 cells producing **(b)** WT Prp8-3HAp or **(c)** Δ NLS Prp8-3HAp. Glycerol gradient fractions were precipitated with anti-HA agarose and the precipitates were western blotted and probed with anti-Aar2p, anti-Myc, and anti-Snu114p antibodies. **(d)** Immunoprecipitation of Aar2p from splicing extracts derived from KL1-Aar2 producing WT Prp8p (lane 2) or Δ NLS-Prp8p (lane 4). Extracts were incubated with IgG-agarose and precipitated RNAs were analyzed by Northern blotting, probing for U5 snRNAs. Lanes 1 and 3 show 25% of the amount of extract used for each IP.



Snu114p. Stripping the blot and reprobing with anti-Prp8p antibodies showed that Prp8p was associated with Brr2p only in the heavier fractions (1 to 11, not shown), in agreement with the Prp8p pull down of Brr2p (**Fig. 2b**). Thus, in addition to the Brr2p that is complexed with Prp8p and Snu114p in mature U5 snRNPs, there is a pool of Brr2p that is not associated with either Snu114p or Prp8p. It will be interesting to determine whether the latter form of Brr2p is complexed with other proteins, such as the U5 snRNP proteins, Snu40p, Prp28p and Dib1p.

The proposal that the Aar2p-Prp8p complex is in equilibrium with the Brr2p-Prp8p complex also predicts that this equilibrium might be disturbed by altering the availability of Brr2p. To test this, strain RG-MetB2-8T was constructed, in which expression of *BRR2* is repressed by methionine and Prp8 is TAP-tagged. Addition of methionine to the growth medium causes cell growth to slow substantially after about 10 hours (**Fig. 3b**) as a consequence of Brr2p-depletion. Prp8-TAP precipitation followed by western blotting showed that at 6.5 and 10 hours following addition of methionine, as Brr2p became depleted, less Brr2p and more Aar2p was co-precipitated with Prp8-TAP, whereas the amount of Snu114p associated with Prp8-TAP was similar (**Fig. 3c**). This strongly supports an equilibrium between the Aar2p-Prp8p and Brr2p-Prp8p complexes.

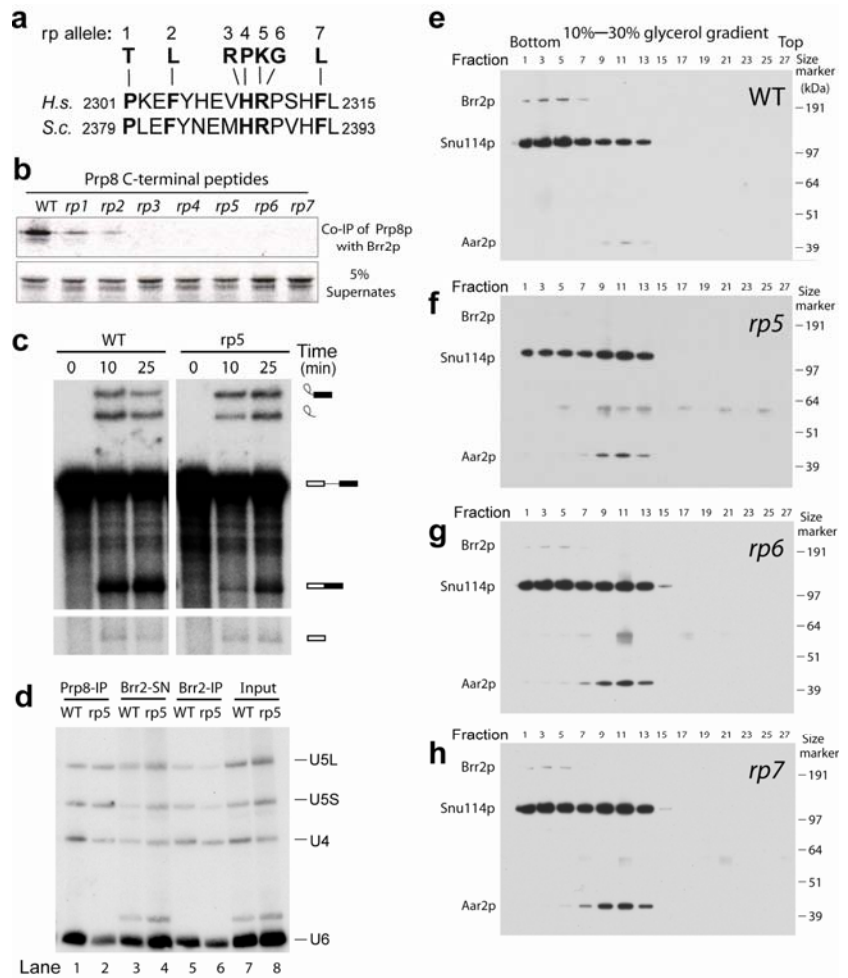


U5 snRNP maturation and Retinitis pigmentosa

As all of the RP-causing mutations affect amino acids in the extreme C-terminus of hPrp8, a region that is highly conserved from yeast to human, we investigated the effects of some of these mutations in the budding yeast Prp8p. Seven missense mutations were tested, each changing an amino acid that is identical in human and budding yeast Prp8p. We previously demonstrated a two-hybrid interaction between the C-terminus of Prp8p and Brr2p³⁰. This interaction was disrupted by the yeast *prp8-1* mutation which affects the same region of Prp8p as the RP mutations³⁰. We therefore used an *in vitro* binding assay to investigate the effects of seven missense RP mutations³ (referred to hereafter as *rp1-7*; **Fig. 4a**), on the association of a C-terminal Prp8 peptide with Brr2p. Residues 2210 to 2413 of yeast Prp8p were identified as the minimum region for the interaction with Brr2p, although the interaction was strengthened with a longer peptide (**Supplementary Fig. 2**). The ³⁵S-methionine-labeled 204 amino acid peptides were produced by *in vitro* translation and incubated with yeast cell extract containing full-length Myc-tagged Brr2p and anti-Myc antibodies. Compared to the wild-type Prp8 peptide, all seven *prp8-rp* mutations that were tested reduced or eliminated the association with Brr2p (**Fig. 4b**). Similarly, Pena et al.³¹ recently showed, using a two-hybrid assay in yeast, that some of the same RP mutations when present in the C-terminus of hPrp8 disrupted its interaction with hBrr2 and/or with hSnu114. Thus, the molecular defect(s) caused by the RP mutations may be conserved from yeast to man.

Figure 3 Analysis of Brr2 interactions. **(a)** Splicing extract from glucose-grown KL1-BRR2 cells carrying pJU204-noHA (Brr2-TAP, untagged Prp8) was glycerol gradient fractionated, precipitated with IgG-agarose, and the precipitates were analyzed by western blotting, probing with anti-Snu114p antibodies. **(b)** RG-B64-8T cells (Prp8-TAP), and RG-MetB2-8T cells (Prp8-TAP and *P_{MET}-BRR2*) were grown under inducing conditions (no methionine) and then methionine was added to 10 mM to repress *BRR2* expression. Cell extracts were prepared at 0, 6.5 and 10 hours following addition of methionine (vertical arrows). **(c)** Extracts prepared as in panel b were incubated with IgG-Sepharose beads and the pellets were analyzed by western blotting, probing with anti-Brr2, anti-Snu114 and anti-Aar2 antibodies.

Figure 4 Effects of *prp8-rp* mutations. **(a)** Amino acid sequence alignment of a region near the C-terminus of Prp8p from human (*H.s.*) and *S. cerevisiae* (*S.c.*), indicating the positions of the *rp* mutations that were tested in this work. The numbers indicate the positions of this region in the proteins. **(b)** Effect of the *rp* mutations on co-precipitation of C-terminal fragments of Prp8p with Brr2p. ³⁵S-methionine-labeled peptides corresponding to aa 2210–2413 from the C-terminus of yeast Prp8p, and containing the wild-type or *rp1–7* mutant sequence as indicated, were mixed with yeast extract containing N-terminally tagged Myc-Brr2p. Immunoprecipitation of Myc-Brr2p followed by gel electrophoresis and autoradiography shows the level of Prp8p peptide association. **(c)** The *rp5* mutation affects splicing activity *in vitro*. Splicing extracts from KL1 cells producing wild-type (WT) Prp8p or Prp8-*rp5* protein were assayed for splicing activity⁴³ at 24°C using *ACT1* RNA as substrate. After 10 or 25 min incubation the reaction products were fractionated in a 7% denaturing polyacrylamide gel and visualized by autoradiography. The positions of pre-mRNA, intermediates and products of the reactions are illustrated on the right side. **(d)** Cultures of KL3-BRR2 producing WT Prp8p or Prp8-*rp5* mutant protein were grown on glucose medium at 30°C and shifted to 37°C for 30 min. Splicing extracts were prepared and incubated with anti-Prp8 antibodies (lanes 1 and 2) or with anti-Brr2 antibodies (lanes 3–6). RNA was extracted from the precipitates (IP; lanes 1, 2, 5, 6), from 20% of the anti-Brr2 unbound fractions (Brr2-SN; lanes 3 and 4) and 10% of total extract (input; lanes 7 and 8) and snRNAs were analyzed by Northern blotting. **(e–h)** Splicing extracts from WT, *rp5*, *rp6* and *rp7* strains (KL3-Brr2 carrying pJU204, pKL-*rp5*, pKL-*rp6* or pKL-*rp7*) grown at 30°C were glycerol gradient fractionated, immunoprecipitated with anti-HA agarose, and the precipitates were western blotted, probing with anti-Aar2, anti-Myc, and anti-Snu114 antibodies.



We then created yeast strains that express these seven *prp8-rp* alleles, by introducing the mutations either into the chromosomal *PRP8* gene or into *PRP8* on a plasmid in a strain in which the chromosomal gene was fully repressed in glucose medium. The *rp* strains made by the two approaches gave similar results. The *rp1* (P2379T), *rp2* (F2382L), *rp3* (H2387R) and *rp4* (H2387P) mutant strains behaved in an unstable manner, displaying variable colony sizes, and the *rp3* and *rp4* mutants failed to grow at 37°C. The *rp5* (R2388K) and *rp6* (R2388G) alleles supported good growth at 23°C but poor or no growth at higher and lower temperatures, whereas *rp7* (F2392L) caused a mild growth defect at 14°C to 18°C. As the *rp5*, *rp6* and *rp7* mutants displayed more stable phenotypes they were selected for further analysis. The presence of the 3HA-tag at the C-terminus of Prp8p exacerbated the growth defects of the *rp* mutants compared to untagged *rp* alleles (data not shown; A. Kutach & C. Guthrie, University of California, San Francisco, personal communication). This is intriguing in view of the fact that one of the reported RP mutations alters the stop codon of human PRPF8, extending the open reading frame by 41 amino acids²⁰. Although the addition of a C-terminal 3HA tag does not cause an obvious growth or splicing defect with wild-type yeast Prp8p, it may enhance the RP phenotype of *prp8-rp* mutants by effectively combining two *rp* alleles. The extended sequence might further weaken the interaction of the C-terminus of Prp8p with Brr2p, when it is already weakened by the *rp1–7* point mutations. In all experiments the tagged mutants were compared to tagged wild-type. However, the C-terminal peptide used in the *in vitro* pull-down experiment (Fig. 4b) was not tagged.

When extracts from *prp8-rp5* cells were tested for the ability to splice *in vitro*, the rate of *ACT1* pre-mRNA splicing was slower than in wild-type extracts (Fig. 4c). In addition, there was a severe splicing defect when reactions were incubated at both lower and higher temperatures (Supplementary Fig. 3). Thus the *in vitro* splicing activity showed the same heat and cold sensitivity as growth of the *prp8-rp5* mutant cells. RT-PCR analysis showed a defect in the splicing of *ACT1* transcripts *in vivo* in *rp5* and *rp6* cells grown at 30°C, that increased substantially at 37°C (Supplementary Fig. 4). In addition, microarray analysis showed a genome-wide splicing defect for *rp5* mutant cells incubated at 14°C or 37°C and for *rp6* mutant cells incubated at 37°C, confirming a general splicing defect *in vivo* (Supplementary Fig. 5).

To investigate the effect of the *rp5* mutation on the association of Prp8p and Brr2p with snRNPs, extracts from wild-type and *rp5* mutant cells were incubated with anti-Prp8p or anti-Brr2p antibodies and the co-precipitated snRNAs were detected by northern analysis. Mutant and wild-type Prp8p were associated with similar levels of U5 snRNAs but mutant Prp8p brought down less U4 and U6 snRNAs, indicating a defect in the incorporation of mutant Prp8p into U4/U6.U5 tri-snRNPs (Fig. 4d, lanes 1 and 2). In contrast, Brr2p was associated with less U4, U5 and U6 snRNAs in the mutant compared with the wild-type, but the difference was more pronounced for the U5 snRNAs (Fig. 4d, lanes 5 and 6). This is supported by the amounts of snRNAs that were unbound (Fig. 4d, lanes 3 and 4), and suggests a defect in the association of Brr2p with U5 snRNA in the mutant strain, with most or all of the mutant U5 snRNPs

that do contain Brr2p being incorporated into tri-snRNPs. These results strongly suggest that although the *rp5* mutation does not prevent the association of mutant Prp8p with U5 snRNA, it causes a defect in the formation of Brr2-containing U5 snRNPs, resulting in reduced amounts of U4/U6.U5 tri-snRNP complexes, which would explain the reduced splicing efficiency.

Extracts from the *prp8-rp* mutation strains were fractionated in glycerol gradients followed by immuno-precipitation of Prp8p and western blot analysis. Compared to wild-type Prp8p (Fig. 4e), the Prp8-rp mutant proteins were associated with less Brr2p (Fig. 4f, g and h, lanes 1–7) and with more Aar2p (Fig. 4f, g and h, lanes 9–13). Also, in the mutant extracts the distribution of Prp8-associated Snu114p was different, with less present in the high density fractions compared to wild-type. The effect of the *prp8-rp5* mutation on Brr2p associations was then investigated in a similar way. Strikingly, extract from the mutant strain showed more Brr2p in the lighter gradient fractions and less Snu114p co-precipitating with Brr2p from the denser fractions (Supplementary Fig. 6). As expected, no Aar2p was detected in any of the Brr2p precipitates. This supports the conclusion that the *prp8-rp5* mutation causes reduced incorporation of Brr2p into U5 snRNPs and larger snRNP complexes.

The effects of the *prp8-rp* mutations on snRNP formation and splicing resemble those of the *prp8ΔNLS* mutation. We therefore used immunofluorescence microscopy to investigate the localization of the yeast Prp8-rp mutant proteins. However, unlike the Δ NLS-Prp8p, the Prp8-rp mutant proteins showed no sign of delocalization from the nucleus (data not shown). Thus the Prp8p-Aar2p complex that accumulates in the *prp8-rp* mutants is nuclear and therefore, unlike the situation with Δ NLS-Prp8p, has the possibility to interact with Brr2p but does so with reduced efficiency as a consequence of the poor association of Brr2p with Prp8-rp mutant proteins.

DISCUSSION

Our data confirm the existence of two distinct U5 snRNP complexes, and suggest that U5 snRNP biogenesis has a cytoplasmic phase in yeast as it does in metazoan cells. Although the association of Prp8p with cytoplasmic U5 snRNP precursor particles has not been noted in metazoan cells, considering the high conservation of the U5 snRNP components (especially of Prp8p), it seems likely that the pathway of U5 snRNP biogenesis is also conserved. Indeed, a role for Prp8p in the nuclear uptake of U5 snRNP precursor particles could explain why this process is m₃G cap independent in *Xenopus* oocytes³². Within the nucleus, the conversion of U5 precursor to mature U5 snRNP involves substitution of Aar2p at the C-terminus of Prp8p by Brr2p, and presumably the acquisition of the other three U5-specific proteins (Prp28p, Snu40 and Dib1p). The RP mutations residing in the C-terminus of Prp8p interfere with U5 snRNP maturation in a different manner to the N-terminal Δ NLS mutation, causing a defect in the interaction of Prp8p with Brr2p, thereby reducing functional U5 snRNP and U4/U6.U5 tri-snRNP formation in the nucleus (Fig. 5). Although a precursor-product relationship between the Aar2-U5 complex and the Brr2-U5 snRNP has not been formally demonstrated, such a relationship is strongly suggested by the finding that 1) the amount of Aar2p-Prp8p complex is increased and the amounts of Brr2p-Prp8p complex and of U4/U6.U5 tri-snRNP complex are decreased as a consequence of the *prp8ΔNLS* or the *prp8-rp* mutations, 2) the amount of a novel form of Brr2p that is not Prp8-associated is increased by the *prp8-rp5* mutation, and 3) the metabolic depletion of Brr2p also causes an accumulation of Aar2p-Prp8p complex.

We showed previously³³ that the region of Prp8p encompassed by aa 771–2413 associates with Aar2p and that dissection of Prp8p at aa 2173 by expressing it as two separate polypeptides disrupts its association with Aar2p. Therefore,

Aar2p may interact with the C-terminus of Prp8p in close proximity to the region of Brr2p interaction.

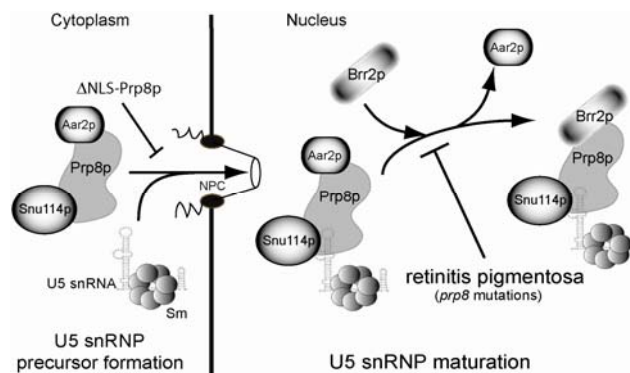


Figure 5 Cartoon showing the proposed pathway for U5 snRNP biogenesis in budding yeast. Note that the U5 snRNP proteins Prp28p, Snu40 and Dib1p are not shown. Their interactions were not investigated in this work but, based on the reported compositions of the Aar2- and Brr2-containing particles^{25,26}, they are assumed to join the U5 snRNP in the nucleus at the same stage as Brr2p. NPC, nuclear pore complex; Sm, a complex of 7 core snRNP proteins.

This suggests a potential model for a competitive interaction of Aar2p and Brr2p with Prp8p. Presumably, Aar2p plays an as yet unknown but important role in the biogenesis of U5 snRNPs, possibly as a chaperone to control the assembly of the mature particle. Therefore the cytoplasmic location for the formation of the precursor U5 particle may be a critical feature of U5 snRNP biogenesis, ensuring that Aar2p associates with Prp8p before it is exposed to Brr2p in the nucleus. Indeed, Kutach and Guthrie (personal communication) have evidence that the prior binding of Aar2p to a C-terminal fragment of Prp8p inhibits the subsequent association of Prp8p with Brr2p *in vitro*. These observations support the hypothesis that the *rp* defect is a consequence of decreased affinity of Brr2p for a mutated C-terminus of Prp8 that results in a defect in the production of mature U5 snRNPs in the nucleus. This further suggests that the normal equilibrium between the Aar2-U5 and the Brr2-U5 snRNP complexes depends, at least in part, on this Prp8p-Brr2p interaction.

The reduced splicing activity in yeast carrying the *rp* mutations (Fig. 4c) is likely to be a direct consequence of the reduction in level of mature U5 snRNPs. This is presumably the earliest defect in the splicing pathway that is caused by the RP mutations. However, the incorporation of mutant Prp8p into spliceosomes may also affect spliceosome activation by Brr2p and might explain the observed temperature sensitivity of growth and of splicing caused by some of the RP alleles.

Could this reduced splicing activity explain the clinical consequences of RP in human patients? The first symptoms of RP are night blindness and loss of peripheral vision, generally beginning in childhood. RP is therefore a late-onset, progressive, degenerative disease rather than a developmental defect. The retina is a complex, specialized, non-dividing tissue with high oxygen consumption and an unusually large number of mitochondria, implying a high metabolic rate (reviewed by³⁴). Rod and cone photoreceptors turn over their outer segments daily, which is likely to require a high level of expression of both retina specific and housekeeping genes during a particular period early each day. Therefore, a reduced level of splicing activity may have a cumulative effect which has much more serious consequences in these cells than in other tissues.

However, mutations causing human inherited disease have been identified in other components of the splicing machinery³⁵, each of which may also cause mild splicing defects, and it is unclear what makes the effect of the *rp* mutations retina specific. The fact that these cause a dominant genetic defect in humans may offer a clue. The *rp5* and *rp6* mutations did not cause a dominant growth defect in heterozygous diploid yeast (data not shown). Therefore, the dominant aspect of the disease may be specific to retinal cells. How could our model explain dominance? The accumulation of the Aar2-U5 snRNP in the nucleus might cause a dominant defect if it became inappropriately incorporated into tri-snRNPs or spliceosomes. Alternatively, accumulation of defective Aar2-U5 snRNP might sequester a specific factor required for its conversion to the mature U5 snRNP. Also, this factor may be limiting in retinal cells, or the splicing of certain retinal-specific transcripts may involve a retinal-specific factor (in particular a U5 snRNP or U4/U6.U5 tri-snRNP component) that is more sensitive to this defect. It will be important to further characterize the process of U5 snRNP maturation and the specific function of the Aar2 protein. In the meantime, the results presented here explain how RP mutations can cause a splicing defect and suggest testable hypotheses for the molecular basis of splicing factor RP in human cells.

METHODS

Yeast strains and plasmids. Yeast strains and plasmids used in this work are listed in Table 1. Oligonucleotides are in **Supplementary Table 1**. pKLANLS was constructed by deleting codons 96–117 via site-directed mutagenesis of *PRP8* in pJU204²⁷, using oligos F-NLS-P8-352 and R-NLS-P8-285. Strain KL1 has a chromosomal *P_{GAL1}-GST-prp8Δaal1-78* allele that encodes Prp8p with the non-essential N-terminal proline-rich region (aa 1–78) missing, thereby allowing use of anti-8.6 antibodies³³ to detect only plasmid-encoded Prp8p. KL1 and KL3 cannot grow in glucose medium in the absence of plasmid-encoded *PRP8*, as the chromosomal *PRP8* is strongly repressed. KL1 and KL3 were generated from BMA38a by one-step PCR gene replacement using pFA6a-kanMX6-pGAL1-GST or pFA6a-TrpMX6-pGAL1-GST as template³⁶. Strains KL1-Snu114, KL1-Brr2, and KL1-Aar2 were derived from KL1, and KL3-Brr2 was derived from KL3 by one-step PCR³⁷. The C-terminus of *PRP8* (encoding aa 2173–2413 plus 3HA tag) from pJU204 was cloned next to a hygromycin B marker (Hph^r) in pC8HH. By site-directed mutagenesis two series of *rp* mutant plasmids were produced in pC8HH (pC8HH-(rp1–7)) and in pJU204 (pKCL-rp5–7). The RP mutations were introduced into the genomic *PRP8* locus of YCL46³⁸ by one-step PCR from pC8HH plasmids using Hph^r as marker.

Microscopy. GFP fluorescence was detected in BMA38a cells carrying either pGFP-N-FUS39 or pGFP-N-NLS and grown in SD-Ura-Met. Immunofluorescence microscopy. Cells grown to OD₆₀₀ 0.3 to 0.5 were fixed with 1/10 volume 37% (v/v) formaldehyde for 30 min, washed 3 times with buffer B (0.1 M potassium phosphate pH 7.0, 1.2 M sorbitol) and resuspended in 0.5 ml buffer B with lyticase for 30 min at 30°C. Cells were collected and washed once with buffer B. Fixed cells were immobilized on poly-L-lysine coated microscope slides, blocked with 5% (w/v) milk in PBST (PBS with 0.1% (v/v) Tween 20), and incubated overnight at 4°C with antibodies (anti-HA 1:1000, Roche, or anti-protein A 1:10000, Sigma) in a humid chamber. After washing with PBST six times for anti-protein A antibodies or three times for anti-HA antibodies, cells were incubated with Alexa Fluor 594 secondary antibodies (Molecular Probes, Eugene, OR) for 1 h at 23°C in the dark, washed with PBST as before, then mounted with DAPI. Images were obtained using a Leica DMRA2 microscope with CoolSnap HQ cooled CCD camera (Roper Scientific) and LeicaFW400 software (Leica)^{40,41}.

RNA fluorescent in situ hybridisation. The method was adapted from the Singer lab protocol (http://www.singerlab.org/protocols/insitu_yeast.htm). Yeast cells were grown in 36 ml cultures to early log phase (OD₆₀₀ between 0.2–0.4) then fixed for 10 min at RT by directly adding to the medium 8 ml of 20% (v/v) formaldehyde, 50% (v/v) acetic acid. The fixative was removed by three rounds of washing with 10 ml ice-cold buffer B and centrifugation (5 min at 1,100 g, 4°C). Cells were spheroplasted as described above under Microscopy, centrifuged 2 min at 1,100 g and 4°C, and washed once with ice-cold buffer B. Cells were resuspended in 500 µl buffer B,

and 100 µl was added to a poly-L-lysine coated slide and left to adhere by incubating 30 min at 40°C. Slides were washed once with ice-cold buffer B, and stored in 70% (v/v) ethanol at –20°C. Hybridization: Cells were re-hydrated for 5 min in 2x SSC (300 mM NaCl, 30 mM sodium citrate, pH 7.0) and 50% (v/v) formamide, then hybridized overnight at 37°C in 40 µl of a mixture containing 10% (w/v) dextran sulfate, 0.02% (w/v) RNase-free BSA, 40 µg E. coli tRNA, 2x SSC, 50% (v/v) formamide, 1 µl RNasin and 1 µl probe (10 ng). Cells were washed twice for 30 min in 2x SSC, 50% (v/v) formamide at 37°C (U2 probe) or 45°C (U5 and U6 probes) then mounted with Vectashield containing DAPI. The U1 and U2 FISH probes were as described⁴². U2, U5, and U6 FISH probes were 5' Cy3 modified oligos as listed in **Supplementary Table 2**.

Immunoprecipitation, northern analysis of snRNAs and glycerol gradient fractionation. Yeast cell extracts were prepared²⁷ and splicing reactions were performed⁴³ using as substrate ³²P-labeled p283 (*ACT1*) transcript produced by in vitro transcription. Immunoprecipitation of snRNPs and spliceosomes was performed using rabbit anti-Prp8p polyclonal antibodies (anti-8.6³³) and washes containing 150 mM NaCl. The immunoprecipitates were deproteinized by SDS/proteinase K treatment and phenol:chloroform:isoamylalcohol extraction, and the RNA was fractionated on a 6% polyacrylamide gel. ³²P-end-labeled oligonucleotides used to detect snRNAs in Northern blotting are listed in **Supplementary Table 1**. Levels of snRNAs were quantified using a Storm Phosphorimager (GE Healthcare).

Glycerol gradients were made and run essentially as described⁴⁴. Briefly, splicing extracts (80 µl) were diluted with 120 µl GG buffer (20 mM HEPES at pH 7.0, 100 mM KCl, 0.2 mM EDTA; final glycerol concentration 8% (v/v)), sedimented through a 10–30% (v/v) linear glycerol gradient at 243K g for 15 or 17 h in a SW40 Ti rotor (Beckman) at 4°C, and 400 µl fractions were collected³³. Alternate fractions were incubated with 25 µl anti-HA agarose overnight, with mixing at 4°C. The precipitates were fractionated in a 4–12% polyacrylamide gel, blotted and probed with anti-Aar2²⁵, anti-Snu114⁴⁵, anti-Brr2 (against an N-terminal peptide) and/or anti-Myc antibodies (Santa Cruz Biotech.).

Prp8 peptide co-immunoprecipitation. Sequences that encode amino acids 2210–2413 from the C-terminus of Prp8p, with and without the *rp* mutations, were amplified by PCR from plasmids pC8HH-(rp1–7). The ³⁵S-methionine labeled Prp8 peptides were produced using the 'TnT T7 quick for PCR DNA' kit (Promega). The protein interaction assay contained 25µl of yeast extract from strain BCQ1 (over-producing Myc-Brr2p), 5µl of ³⁵S-labeled TnT reaction, 8µl of mouse monoclonal 9E10 anti-Myc antibody (Roche) and 10 mg of protein A-Sepharose, in a total volume of 300µl of buffer (12 mM HEPES pH 7.9, 150 mM NaCl, 5 mM MgCl₂, 0.1% (v/v) NP-40), incubated with mixing for 1 h at 4°C. The pellets were washed with 50 mM Tris pH7.5, 150 mM NaCl and 0.1% (v/v) NP-40, then resuspended in SDS loading buffer, separated by electrophoresis in an 8% SDS polyacrylamide gel and the gels were dried and exposed for autoradiography.

ACKNOWLEDGEMENTS

We thank P. Fabrizio (Max Planck Institute, Göttingen) for the very generous gift of anti-Aar2p and anti-Snu114p antibodies, Olivier Cordin (University of Edinburgh) for anti-Brr2p anti-peptide antibodies, M. Spiller for assistance with immuno-fluorescence staining and microscopy, A. Kutach and C. Guthrie for sharing information prior to publication, and Ilan Davis, Martin Reijns and David Tollervey for critical comments. This work was funded by studentships from The Darwin Trust of Edinburgh to K-L.B. and to T.A. and by Wellcome Trust Grants 067311 (J.D. Beggs) and 073988 (C.F.I.) and European Commission grant LSH-2004-518238 (EURASNET Network of Excellence). J.D.B. is the Royal Society Darwin Trust Professor.

AUTHOR CONTRIBUTIONS

K-L.B. contributed the data for Figs. 1, 2, 4c, e–h, and Supplementary Figs. 1, 3 and 6; R.J.G. contributed the data for Figs. 3b, c and 4b and Supplementary Fig. 2, S1; P.E. contributed Fig. 4d and investigated the effects of HA-tagging Prp8p with and without the *rp* mutations (data not shown); J.D. Barrass performed the RT-PCR and microarray analyses (Supplementary Fig. 4 and 5); T.A. contributed Fig. 3a; C.F.I. provided expertise on Retinitis pigmentosa; J.D. Beggs supervised all this work and wrote most of the paper.

- Will, C.L. & Lührmann, R. Spliceosomal UsnRNP biogenesis, structure and function. *Curr. Opin. Cell Biol.* **13**, 290-301 (2001).
- Jurica, M.S. & Moore, M.J. Pre-mRNA splicing: awash in a sea of proteins. *Mol Cell* **12**, 5-14 (2003).
- McKie, A.B. *et al.* Mutations in the pre-mRNA splicing factor gene PRPC8 in autosomal dominant retinitis pigmentosa (RP13). *Hum. Mol. Genet.* **10**, 1555-1562 (2001).
- Vithana, E.N. *et al.* A human homolog of yeast pre-mRNA splicing gene, PRP31, underlies autosomal dominant retinitis pigmentosa on chromosome 19q13.4 (RP11). *Mol Cell* **8**, 375-381 (2001).
- Chakarova, C.F. *et al.* Mutations in HPRP3, a third member of pre-mRNA splicing factor genes, implicated in autosomal dominant retinitis pigmentosa. *Hum. Mol. Genet.* **11**, 87-92 (2002).
- Keen, T.J. *et al.* Mutations in a protein target of the Pim-1 kinase associated with the RP9 form of autosomal dominant retinitis pigmentosa. *Eur. J Hum. Genet.* **10**, 245-249 (2002).
- Maita, H. *et al.* PAP-1, the mutated gene underlying the RP9 form of dominant retinitis pigmentosa, is a splicing factor. *Experimental Cell Research* **300**, 283-296 (2004).
- Kiss, T. Biogenesis of small nuclear RNPs. *J Cell Sci* **117**, 5949-5951 (2004).
- Bertrand, E. & Bordonne, R. Assembly and traffic of small nuclear RNPs. *Prog. Mol. Subcell. Biol* **35**, 79-97 (2004).
- Yong, J., Wan, L., & Dreyfuss, G. Why do cells need an assembly machine for RNA-protein complexes? *Trends Cell. Biol.* **14**, 226-232 (2004).
- Huber, J. *et al.* Snurportin1, an m3G-cap-specific nuclear import receptor with a novel domain structure. *EMBO J* **17**, 4114-4126 (1998).
- Jantsch, M.F. & Gall, J.G. Assembly and localization of the U1-specific snRNP C protein in the amphibian oocyte. *J. Cell Biol.* **119**, 1037-1046 (1992).
- Romac, J.M.J., Graff, D.H., & Keene, J.D. The U1 small nuclear ribonucleoprotein (snRNP) 70k protein is transported independently of U1 snRNP particles via a nuclear localization signal in the RNA-binding domain. *Mol. Cell Biol.* **14**, 4662-4670 (1994).
- Hetzer, M. & Mattaj, J.W. An ATP-dependent, Ran-independent Mechanism for Nuclear Import of the U1A and U2B" Spliceosome Proteins. *J. Cell Biol.* **148**, 293-304 (2000).
- Nesic, D., Tanackovic, G., & Kramer, A. A role for Cajal bodies in the final steps of U2 snRNP biogenesis. *J Cell Sci* **117**, 4423-4433 (2004).
- Ohno, M., Segref, A., Bachi, A., Wilm, M., & Mattaj, J.W. PHAX, a Mediator of U snRNA Nuclear Export Whose Activity Is Regulated by Phosphorylation. *Cell* **101**, 187-198 (2000).
- Grainger, R.J. & Beggs, J.D. Prp8 protein: at the heart of the spliceosome. *RNA* **11**, 533-557 (2005).
- Jackson, S.P., Lossky, M., & Beggs, J.D. Cloning of the RNA8 gene of *Saccharomyces cerevisiae*, detection of the RNA8 protein, and demonstration that it is essential for nuclear pre-mRNA splicing. *Mol. Cell Biol.* **8**, 1067-1075 (1988).
- Lou, H.R., Moreau, G.A., Levin, N., & Moore, M.J. The human Prp8 protein is a component of both U2- and U12-dependent spliceosomes. *RNA* **5**, 893-908 (1999).
- Martinez-Gimeno, M. *et al.* Mutations in the pre-mRNA splicing-factor genes PRPF3, PRPF8, and PRPF31 in Spanish families with autosomal dominant retinitis pigmentosa. *Invest Ophthalmol. Vis. Sci* **44**, 2171-2177 (2003).
- Kondo, H. *et al.* Diagnosis of Autosomal Dominant Retinitis Pigmentosa by Linkage-Based Exclusion Screening with Multiple Locus-Specific Microsatellite Markers. *Invest. Ophthalmol. Vis. Sci.* **44**, 1275-1281 (2003).
- Ziviello, C. *et al.* Molecular genetics of autosomal dominant retinitis pigmentosa (ADRP): a comprehensive study of 43 Italian families. *J. Med. Genet.* **42**, e47 (2005).
- Testa, F. *et al.* Clinical phenotype of an Italian family with a new mutation in the PRPF8 gene. *Eur. J. Ophthalmol.* **16**, 779-781 (2006).
- De Erkenez, A.C., Berson, E.L., & Dryja, T.P. Novel mutations in the PRPC8 gene, encoding a pre-mRNA splicing factor in patients with autosomal dominant Retinitis Pigmentosa. ARVO, online abstract. (2002)
- Gottschalk, A., Kastner, B., Lührmann, R., & Fabrizio, P. The yeast U5 snRNP coisolated with the U1 snRNP has an unexpected protein composition and includes the splicing factor Aar2p. *RNA* **7**, 1554-1565 (2001).
- Stevens, S.W. *et al.* Biochemical and genetic analysis of the U5, U6, and U4/U6.U5 small nuclear ribonucleoproteins from *Saccharomyces cerevisiae*. *Proc. Natl. Acad. Sci. USA* **7**, 1543-1553 (2001).
- Umen, J.G. & Guthrie, C. A novel role for a U5 snRNP protein in 3' splice site selection. *Genes Dev.* **9**, 855-868 (1995).
- Bordonne, R. Functional characterization of nuclear localization signals in yeast Sm proteins. *Mol Cell Biol* **20**, 7943-7954 (2000).
- Achsel, T., Ahrens, K., Brahms, H., Teigelkamp, S., & Lührmann, R. The human U5-220kD protein (hPrp8) forms a stable RNA-free complex with several U5-specific proteins, including an RNA unwindase, a homologue of ribosomal elongation factor EF-2, and a novel WD-40 protein. *Mol Cell Biol.* **18**, 6756-6766 (1998).
- van Nues, R.W. & Beggs, J.D. Functional contacts with a range of splicing proteins suggest a central role for Brr2p in the dynamic control of the order of events in spliceosomes. *Genetics* **157**, 1451-1467 (2001).
- Pena, V., Liu, S., Bujnicki, J.M., Lührmann, R., & Wahl, M.C. Structure of a multipartite protein-protein interaction domain in splicing factor prp8 and its link to retinitis pigmentosa. *Mol Cell* **25**, 615-624 (2007).
- Fischer, U. *et al.* Diversity in the Signals Required for Nuclear Accumulation of U snRNPs and Variety in the Pathways of Nuclear Transport. *J. Cell Biol.* **113**, 705-714 (1991).
- Boon, K.-L., Norman, C.M., Grainger, R.J., Newman, A.J., & Beggs, J.D. Prp8p dissection reveals domain structure and protein interaction sites. *RNA* **12**, 198-205 (2005).
- Steinberg, R.H. Monitoring communications between photoreceptors and pigment epithelial cells: effects of "mild" systemic hypoxia. Friedenwald lecture. *Invest Ophthalmol. Vis. Sci.* **28**, 1888-1904 (1987).
- Faustino, N.A. & Cooper, T.A. Pre-mRNA splicing and human disease. *Genes Dev.* **17**, 419-437 (2003).
- Longtine, M.S. *et al.* Additional modules for versatile and economical PCR-based gene deletion and modification in *Saccharomyces cerevisiae*. *Yeast* **14**, 953-961 (1998).
- Puig, O., Gottschalk, A., Fabrizio, P., & Seraphin, B. Interaction of the U1 snRNP with nonconserved intronic sequences affects 5' splice site selection. *Genes Dev.* **13**, 569-580 (1999).
- Lesser, C.F. & Guthrie, C. Mutational analysis of pre-messenger RNA splicing in *Saccharomyces cerevisiae* using a sensitive new reporter gene, CUP1. *Genetics* **133**, 851-863 (1993).
- Niedenthal, R.K., Riles, L., Johnston, M., & Hegemann, J.H. Green fluorescent protein as a marker for gene expression and subcellular localization in budding yeast. *Yeast* **12**, 773-786 (1996).
- Carter, K.C. *et al.* A three-dimensional view of precursor messenger RNA metabolism within the mammalian nucleus. *Science* **259**, 1330-1335 (1993).
- Samarsky, D.A., Fournier, M.J., Singer, R.H., & Bertrand, E. The snoRNA box C/D motif directs nucleolar targeting and also couples snoRNA synthesis and localization. *EMBO J* **17**, 3747-3757 (1998).
- Olson, B.L. & Siliciano, P.G. A diverse set of nuclear RNAs transfer between nuclei of yeast heterokaryons. *Yeast* **20**, 893-903 (2003).
- Lin, R.-J., Newman, A.J., Cheng, S.-C., & Abelson, J. Yeast mRNA splicing in vitro. *J. Biol. Chem.* **260**, 14780-14792 (1985).
- Boon, K.-L. *et al.* Yeast Ntr1/Spp382 Mediates Prp43 Function in Postsliceosomes. *Mol. Cell. Biol.* **26**, 6016-6023 (2006).
- Bartels, C., Urlaub, H., Lührmann, R., & Fabrizio, P. Mutagenesis suggests several roles of Snu14p in pre-mRNA splicing. *J Biol Chem.* **278**, 28324-28334 (2003).
- Albers, M., Diment, A., Muraru, M., Russell, C.S., & Beggs, J.D. Identification and characterization of Prp45p and Prp46p, essential pre-mRNA splicing factors. *RNA* **9**, 138-150 (2003).

Supplementary Information

Figure 1. Effect of Δ NLS on (a) co-precipitation of snRNAs with Prp8p and (b) *in vitro* splicing. a) Extracts from YPDA-grown KL1 cells carrying either pJU204 (WT; lanes 1 and 2) or pK Δ NLS (Δ NLS; lanes 3 and 4) were immunoprecipitated with anti-Prp8p antibodies, RNA was extracted from the precipitates and analyzed by Northern blotting, probing for the U4, U5 and U6 snRNAs. Lanes 1 and 3 show 25% of the amount of extract used for each IP. Numbers on the right indicate the efficiency of co-precipitation of each snRNA with Δ NLS-Prp8p compared to WT Prp8p, normalized to the total amount of the snRNAs in each extract. b) Extracts as in (a) were assayed for splicing activity¹ at 24°C using *ACT1* RNA as substrate. The reaction products were fractionated on a 7% denaturing polyacrylamide gel and visualised by autoradiography. The positions of pre-mRNA, intermediates and products of the reactions are illustrated on the right side. M, size markers.

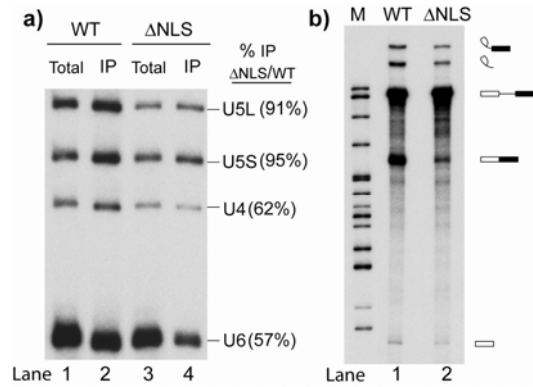
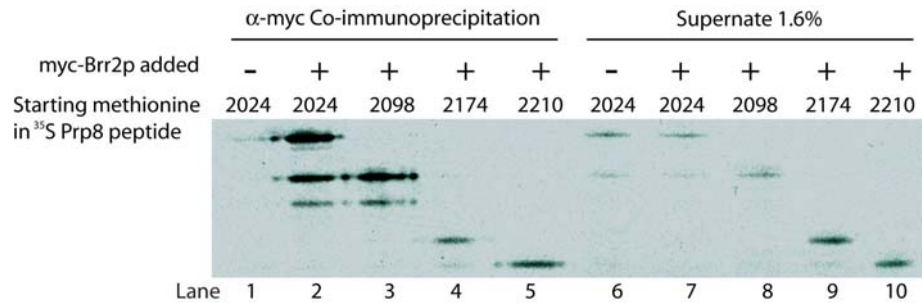


Figure 2. Defining the minimal region of Prp8p that interacts with Brr2p. ³⁵S-methionine-labeled Prp8 C-terminal peptides of different lengths were produced by *in vitro* translation and mixed with yeast extract containing N-terminally tagged Myc-Brr2p. Note that using the Promega ‘TnT T7 quick for PCR DNA’ kit allows protein



synthesis to start at internal methionines, consequently peptides are produced that start at downstream methionines. Lane 1, Prp8 aa 2024–2413 alone (control). Lanes 2–5, Myc-Brr2 extract plus Prp8 peptides starting from amino acids 2024, 2098, 2174 or 2210 respectively. Lanes 6–10, 1.6% of supernates corresponding to samples shown in lanes 1–5. Method: Plasmid pC8HH containing the C-terminus of Prp8 (amino acids 2173–2413) from pJU204 was used to create PCR templates for coupled transcription/translation using the Promega ‘TnT T7 quick for PCR DNA’ kit. Templates that started at methionine codons 2024, 2098, 2174, 2210 or 2413 were used to produce ³⁵S-methionine labeled Prp8 peptides of different lengths, without the HA-tag. Yeast splicing extracts containing high levels of Myc-Brr2p were made from strain BCQ1 by standard methods. The co-immunoprecipitation reaction was carried out in a total volume of 300μl: 10mg of Protein A-Sepharose was added to 25μl of yeast extract, 5μl of TnT reaction (³⁵S) and 8μl of mouse monoclonal 9E10 anti-Myc antibody (Roche). The binding reaction was performed in ice-cold 12 mM HEPES pH 7.9, 150 mM NaCl, 5 mM MgCl₂, 0.1% (v/v) NP-40 and the pellets were washed with 50 mM Tris pH7.5, 150 mM NaCl and 0.1% (v/v) NP-40. The pellets, resuspended in SDS loading buffer, were fractionated in an 8% SDS acrylamide gel, gel was dried and exposed to autoradiography.

Figure 3. The *rp5* mutation affects *in vitro* splicing activity more severely at high and low temperatures. Splicing extracts derived from wild-type (WT; RGY8RP+) and *rp5* mutant (RGY8-*rp5*) cells grown at 30°C were assayed for splicing activity at different temperatures as indicated. The positions of pre-mRNA, intermediates and products of the reactions are illustrated.

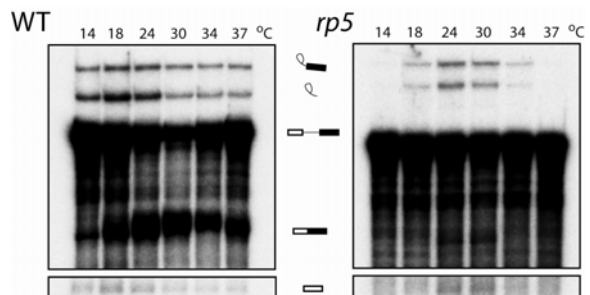


Figure 4. Yeast strains carrying the *rp5* or *rp6* mutation have a splicing defect *in vivo*. RNA was prepared from cultures of wild-type, *rp5* and *rp6* (RGY8RP+, RGY8-*rp5* and RGY8-*rp6*) strains grown at 30°C or 30 min after shifting to 37°C. The presence of unspliced pre-mRNA was detected by quantitative RT-PCR: 1st strand synthesis used a primer specific for the *ACT1* 2nd exon (YFL039C_1_E_R), then QPCR was performed using a pair of primers (YFL039C_1_p_F and YFL039C_1_p_R) that hybridize entirely within the *ACT1* intron. As the PCR product spans the branch point, it is a measure of unspliced intron-containing pre-mRNA. The Ct values for the wild type pre-mRNA were subtracted from the corresponding value for the mutant strains. The relative abundance was calculated as 2 to the power of minus this difference ($2^{-\Delta C_t}$). The values shown therefore represent the percent of the pre-mRNA level in the mutant strain relative to the wild-type strain under the same conditions.

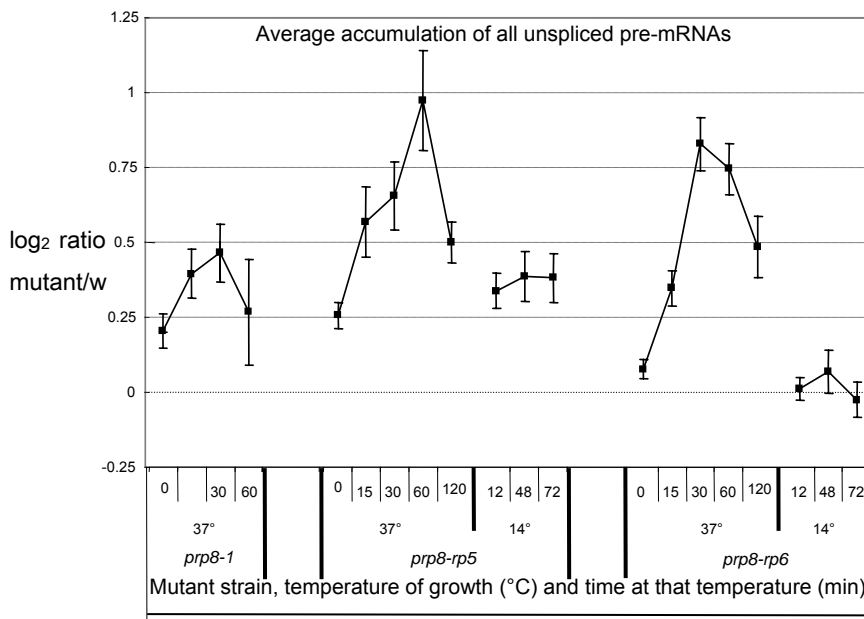
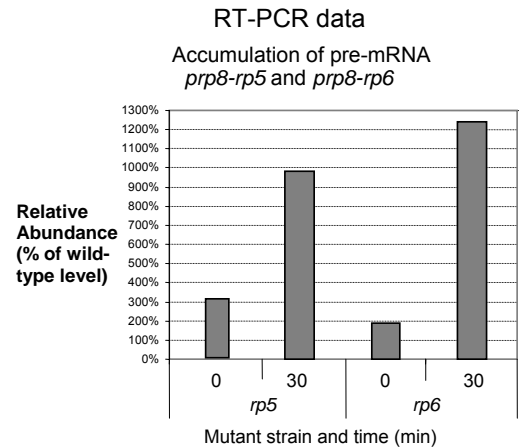


Figure 5. The *rp5* and *rp6* mutation cause a genome-wide splicing defect. Microarray analysis of pre-mRNA splicing was performed using an oligonucleotide microarray that contains probes to detect introns and spliced exon junctions for all the nuclear intron-containing genes in *S. cerevisiae*. It therefore detects accumulation of unspliced pre-mRNAs and depletion of spliced mRNAs genome-wide. The probes were similar in design to those of Clark et al.², and represent 316 introns or putative introns, including predicted alternative splice sites. Wild-type, *prp8-rp5* and *prp8-rp6* strains were grown at 30°C and then shifted to 14°C or 37°C and samples were taken for RNA extraction at the times indicated. Cy3 and Cy5 dye-labeled cDNAs were produced by reverse transcription using a mixture of gene-specific primers complementary to exonic

sequences 3' of the introns. The figure shows a comparison of unspliced pre-mRNA accumulation in the mutant strains relative to wild-type (\log_2 of the ratios), averaging the values for all intron-containing genes on the array (error bars indicate the 95% confidence limit). Cluster analysis of the data revealed that the splicing defects of the *rp5* and *rp6* mutants were more similar to the defects caused by the *prp8-1* temperature-sensitive allele that maps to the same region of *PRP8* than to other splicing mutants (e.g. *prp2-1* or *prp16-2*; data not shown), but did not allow any conclusion to be made about specific effects of the *rp5* and *rp6* mutations on any particular class of genes. Further details, the list of oligonucleotide sequences used as probes and RT primers and the original microarray data can be found at <http://www.biology.ed.ac.uk/research/groups/jbeggs/microarray/>.

Figure 6 Glycerol gradient fractionation of Brr2p complexes.

Splicing extracts from KL1-Brr2 strains expressing wild-type *PRP8* or *prp8-rp5* were fractionated in a 10–30% linear glycerol gradient for 17 h as described in Materials and Methods. The odd-numbered fractions were incubated with 25 μ l IgG-agarose on a rotating wheel overnight, at 4°C. The precipitates were fractionated in a 4–12% PAGE gel, blotted and probed with anti-Aar2 and anti-Snu114 antibodies. The wild-type strain produced two peaks of Brr2p, with Snu114p only co-precipitating with Brr2p from higher density fractions at the bottom of the gradient. Prp8p-*rp5* splicing extract showed a higher proportion of Brr2p in the lower density fractions and less Snu114p co-precipitating with Brr2p from fractions at the bottom of the gradient. Aar2p was not detected in the precipitates.

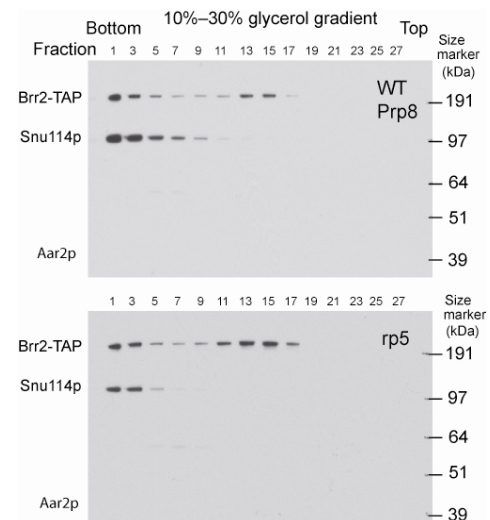


Table 1 Plasmids and yeast strains

| Name | Details | Source |
|---|--|---------------------------------|
| pC8HH | Prp8 aa2173-2413-3HA plus 50nt of 3'UTR from pJU204 cloned into pAG32(Hph) | This work |
| pC8HH rp1-7 | <i>rp</i> mutations inserted into pC8HH | This work |
| pGFP-N-FUS | CEN- <i>URA3-P_{MET25}</i> -GFP | ³ |
| pGFP-N-NLS | CEN- <i>URA3-P_{MET25}</i> -Prp8p-aa96-117-GFP | This work |
| pJU204 | Contains <i>PRP8</i> coding sequence with C-terminal 3HA tag. | ⁴ |
| pJU204-noHA | As pJU204 but with no HA tag | This work |
| pKLΔNLS | pJU204 with <i>PRP8</i> codons 96-117 deleted. | This work |
| pKL-rp5 | <i>PRP8</i> with R2388K in pJU204. | This work |
| pKL-rp6 | <i>PRP8</i> with R2388G in pJU204. | This work |
| pKL-rp7 | <i>PRP8</i> with F2392L in pJU204. | This work |
| pRP3noHA | <i>PRP8</i> with H2387R in pJU204-noHA | This work |
| pRP4noHA | <i>PRP8</i> with H2387P in pJU204-noHA | This work |
| pRP5noHA | <i>PRP8</i> with R2388K in pJU204-noHA | This work |
| pFA6a-kanMX6- <i>P_{GALI}</i> -GST | PCR template for KanMX6- <i>P_{GALI}</i> -GST integration | ⁵ |
| pFA6a- <i>TRP1</i> - <i>P_{GALI}</i> -GST | PCR template for TrpMX6- <i>P_{GALI}</i> -GST integration | ⁵ |
| pFA6a-13Myc-HphMX3 | PCR template for 13-Myc tagging | This work |
| pBS1539 | PCR template for TAP tagging | ⁶ |
| pBS1365 | PCR template for Protein A tagging | ⁶ |
| BMA38a | <i>MATa</i> , <i>his3Δ200</i> , <i>leu2-3,-112</i> , <i>ura3-1</i> , <i>trp1Δ1</i> , <i>ade2-1</i> , <i>can1-100</i> | ⁷ |
| KL1 | <i>Kan-P_{GALI}</i> -GST- <i>prp8Δaal-78</i> , otherwise as BMA38a | Derived from BMA38a |
| KL1-Brr2 | <i>BRR2-TAP:URA3</i> , otherwise as KL1 | '' |
| KL1-Aar2 | <i>AAR2-TAP:URA3</i> , otherwise as KL1 | '' |
| KL1-Snu114 | <i>SNU114-TAP:URA3</i> , otherwise as KL1 | '' |
| KL3 | <i>TRP1-P_{GALI}</i> -GST- <i>PRP8</i> , otherwise as BMA38a | '' |
| KL3-Brr2 | <i>BRR2-13Myc:Hph</i> , otherwise as KL3 | '' |
| RGY8RP+ | <i>MATα cup1Δ::ura3, leu2, ura3, trp1, lys2, ade, PRP8-3HA:Hph, GAL+</i> | Derived from YCL46 ⁸ |
| RGY8-rp5 | <i>MATα cup1Δ::ura3, leu2, ura3, trp1, lys2, ade, prp8-rp5-3HA:Hph, GAL+</i> | '' |
| RGY8-rp6 | <i>MATα cup1Δ::ura3, leu2, ura3, trp1, lys2, ade, prp8-rp6-3HA:Hph, GAL+</i> | '' |
| RG8T | <i>PRP8-TAP:TRP1</i> , otherwise as BMA38a | ⁹ |
| RG-B64-8T | <i>MATa, ura3-1, Δtrp1, ade2-1, leu2-3,112, trp1-1, his3-11,15, PRP8-TAP:URA3</i> | Derived from BMA64n |
| RG-MetB2-8T | <i>MATa, ura3-1, Δtrp1, ade2-1, trp1-1, his3-11,15, PRP8-TAP:URA3, TRP1:MET3_{UAS}MET3_{TATA}-BRR2</i> | Derived from RG-B64-8T |

Table 2 Deoxyoligonucleotides

FISH Probes

U2Fish1 TTGGACATAAACGGCTCGGAAAGACAGGGAAGAGTATGAAGCAAA
U2Fish2 AGAAGACGAGCGAAGAAATCAACAATAAGAGCGCCCCATCCGCACTA
U5Fish1 GGTAAAAGGCAAGAACCATGTTTCGTTATA
U6Fish1 TGATCATCTCTGTATTGTTTCAAATTGACCAAATGTCCA

snRNAs Probes (Northern blotting)

U1 CACGCCTTCCGCGCCGT
U2 CTACACTTGATCTAAGCCAAAAG
U4 AGGTATTCCAAAAATTCCC
U5 AAGTTCCAAAAATATGGCAAGC
U6 ATCTCTGTATTGTTTCAAATTGACCAA

Oligonucleotides used to create pKLΔNLS

F-NLS-P8-352 ATTACATGGAATGACCAAAAAGGCAAAGAGAAGCAATTTATATCTCC
R-NLS-P8-285 CTTTTTGGTCATTCCATGTAATTCTACTTTCTTTTCTGCTTTAGTC

Oligonucleotides used to create pGFP-N-NLS

F-Xba1-aa96-117-Xho1
TGCTCTAGAAAGAGAAAATTGGACATAGGAAAAGATACTTTCGTCCTCGAAAATCAAGAAAGCGTGCAAAAAA
CTCGAGCGG
R-Xba1aa96-117-Xho1
CCGCTCGAGTTTTTTGCACGCTTTCTTGATTTTCGAGTGACGAAAGTATCTTTTCTATGTCCAATTTTCTCTT
TCTAGAGCA

Oligonucleotides used to create pKL-rp5

F-rp5 CTATAATGAGATGCATAAGCCAGTACACTTTTTACAGTTTAGCG
R-rp5 CGCTAAACTGTAAAAAGTGTACTGGCTTATGCATCTCATTATAG

Oligonucleotides used to create pKL-rp6

F-rp6 CTATAATGAGATGCATGGTCCAGTACACTTTTTACAGTTTAGCG
R-rp6 CGCTAAACTGTAAAAAGTGTACTGGACCATGCATCTCATTATAG

Oligonucleotides used to create pKL-rp7

F-rp7 ATGAGATGCATCGTCCAGTACACTTATTACAGTTTAGCG
R-rp7 CGCTAAACTGTAAATAAGTGTACTGGACGATGCATCTCAT

F2-Prp8 and R1-Prp8 were used to PCR the pFA6a-3HA-kanMX6 construct for PRP8 C-terminal 3-HA tagging

F2-Prp8 GCGGGGGACGAAGAGTTAGAGGCCGA ACAATCGATGTATTTAGCCGGATCCCCGGGTTAATTAA
R1-Prp8 ATATCTATGAAATA ACAGATTCCAGTTTATTGGG GAATATATTCAGAATTCGAGCTCGTTTAAAC
F4-Prp8 and R4-(D78Prp8) were used to generate KL1, F4-Prp8 and R4-Prp8 were used to generate KL3
F4-Prp8 GTGCGATTGA ACTTCCTTCC AAAAAAAAAA TAGCGTCAAA GAAAG GAATTCGAGCTCGTTTAAAC
R4-(D78Prp8) TAATTCTACTTTCTTTTCT GCTTTAGTCT CTAATTCATC TAGACC ACGCGGAACCAGATCCGATT
R4-Prp8 GCTGTCTCTTCAAACCAGGAGGTGGGGGCGGTAGTCCACTCAT ACGCGGAACCAGATCCGATT
F-Aar2-TAP and R-Aar2-TAP produce the TAP construct from pBS1539 to the C-terminal of genomic *AAR2*
F-Aar2-TAP GAGCACAACCCTACCATTGTTGGCGTCTCTATTACCAAAGGCCATCCATGGAAAAGAGAAG
R-Aar2-TAP ATCAAGTCAAATACGTTTGTATGATAGCGCCGCACGATGATCGTTATACGACTCACTATAGGG
F-Brr2-TAP and R-Brr2-TAP produce the TAP construct from pBS1539 to the C-terminal of genomic *Brr2*
F-Brr2-TAP TATCTTGACGCAGATAAAGAGTTGTCTTTGAAATAAATGTGAAATCCATGGAAAAGAGAAG
R-Brr2-TAP TATATTGAAATCCATTGATTATCCAGGACTAACAATGATTTTATACGACTCACTATAGGG
F2-Brr2 and R1-Brr2 produce the 13-Mycs construct from pFA6a-13myc-HphMX3 to the C-terminal of genomic *Brr2*
F2-Brr2 TATCTTGACGCAGATAAAGAGTTGTCTTTGAAATAAATGTGAAA CGGATCCCCGGGTTAATTAA
R1-Brr2 TTATATATTGAAATCCATTGATTATCCAGGACTAACAATGATTGAATTCGAGCTCGTTTAAAC
F-Snu114-TAP and R-Snu114-TAP produce the TAP construct from pBS1539 to the C-terminal of genomic *Snu114*
F-Snu114-TAP AGCGCTGAATTATACGCTCAATTAAGAGAAAATGGCTTAGTACCGTCCATGGAAAAGAGAAG
R-Snu114-TAP AATATTGTGGACATATTGCTTAATCTTATGCGCCAAGATTTTCA³⁵TACGACTCACTATAGGG

Oligonucleotides to create templates for *in vitro* production of ³⁵S-Prp8 peptides

F-2121-pC8HH(RP)-Tnt
CTCGAGTAATACGACTCACTATAGGGAGCCACCATGAAAACATAAATATCAA TGCGCAAGGTGAGGAGATAG
R-Prp8-Tnt+ TCAGCTAAATACATCGATTTGTTCCGCC

Oligos used in QPCR of *ACT1* RNA

YFL039C_1_E_R GGCCAAATCGATTCTCAAAA for reverse transcription
YFL039C_1_p_FAGGGGCTTGAAATTTGGAAAAA
YFL039C_1_p_RGCAACAAAAAGAATGAAGCAATCG

REFERENCES FOR SUPPLEMENTARY INFORMATION

1. Lin,R.-J., Newman,A.J., Cheng,S.-C., & Abelson,J. Yeast mRNA splicing in vitro. *J. Biol. Chem.* **260**, 14780-14792 (1985).
2. Clark,T.A., Sugnet,C.W., & Ares,M., Jr. Genomewide Analysis of mRNA Processing in Yeast Using Splicing-Specific Microarrays. *Science* **296**, 907-910 (2002).
3. Niedenthal,R.K., Riles,L., Johnston,M., & Hegemann,J.H. Green fluorescent protein as a marker for gene expression and subcellular localization in budding yeast. *Yeast* **12**, 773-786 (1996).
4. Umen,J.G. & Guthrie,C. A novel role for a U5 snRNP protein in 3' splice site selection. *Genes Dev.* **9**, 855-868 (1995).
5. Longtine,M.S. *et al.* Additional modules for versatile and economical PCR-based gene deletion and modification in *Saccharomyces cerevisiae*. *Yeast* **14**, 953-961 (1998).
6. Puig,O., Gottschalk,A., Fabrizio,P., & Seraphin,B. Interaction of the U1 snRNP with nonconserved intronic sequences affects 5' splice site selection. *Genes Dev.* **13**, 569-580 (1999).
7. Albers,M., Diment,A., Muraru,M., Russell,C.S., & Beggs,J.D. Identification and characterization of Prp45p and Prp46p, essential pre-mRNA splicing factors. *RNA*. **9**, 138-150 (2003).
8. Lesser,C.F. & Guthrie,C. Mutational analysis of pre-messenger RNA splicing in *Saccharomyces cerevisiae* using a sensitive new reporter gene, CUP1. *Genetics* **133**, 851-863 (1993).
9. Boon,K.-L., Norman,C.M., Grainger,R.J., Newman,A.J., & Beggs,J.D. Prp8p dissection reveals domain structure and protein interaction sites. *RNA* **12**, 198-205 (2005).